



**Calhoun: The NPS Institutional Archive**  
**DSpace Repository**

---

Faculty and Researchers

Faculty and Researchers' Publications

---

2016

# Near real-time improved UUV positioning through--The Unscented Kalman Filter approach

Vio, Renato P.; Cristi, Roberto; Smith, Kevin B.

IEEE

---

Renato P. Vio, Roberto Cristi, Kevin B. Smith, "Near real-time improved UUV positioning through--The Unscented Kalman Filter approach". OCEANS 2016 MTS/IEEE Monterey, 19-23 September 2016  
<https://hdl.handle.net/10945/51542>

---

This publication is a work of the U.S. Government as defined in Title 17, United States Code, Section 101. Copyright protection is not available for this work in the United States.

*Downloaded from NPS Archive: Calhoun*



Calhoun is the Naval Postgraduate School's public access digital repository for research materials and institutional publications created by the NPS community. Calhoun is named for Professor of Mathematics Guy K. Calhoun, NPS's first appointed -- and published -- scholarly author.

**Dudley Knox Library / Naval Postgraduate School**  
**411 Dyer Road / 1 University Circle**  
**Monterey, California USA 93943**

<http://www.nps.edu/library>

# Near real-time improved UUV positioning through channel estimation – The Unscented Kalman Filter approach

Renato P. Vio<sup>(1)</sup>, Roberto Cristi, and Kevin B. Smith  
Naval Postgraduate School  
Monterey, USA  
{rperesvi, rcristi, kbsmith}@nps.edu

**Abstract**—The primary objective of this work is to enhance the navigational and positioning accuracy of Unmanned Underwater Vehicles (UUVs) by networking a number of Unmanned Surface Vehicles (USVs) utilizing underwater acoustic modems and acoustic travel time calculations. In a previous work [1], a tracking algorithm based on the Extended Kalman Filter (EKF) was developed presenting satisfactory results, but the assumption of the errors being Gaussian and zero mean at the base of the EKF is violated by the presence of nonlinearities in the measurement equation. In this work, a more suitable approach based on the Unscented Kalman Filter (UKF) is presented and its results compared to the existing approach. A combination of the EKF/UKF with a Smoothing Algorithm was developed and extensively tested with synthetic data. To validate the concepts, the tracking algorithms (EKF and UKF based) were applied to data collected during sea tests that took place in Monterey Bay in August, 2015

**Keywords**—underwater navigation systems, acoustic modems, unscented Kalman filter, acoustic ray tracing.

## I. INTRODUCTION

Even using advanced Inertial Navigation Systems (INS), underwater vehicles need to obtain a position update from a reliable external source regularly to reduce the errors in positioning. By surfacing, an UUV can get a position update using GPS, but this can be time-consuming or undesirable in many applications. Therefore, a technique to accurately update the position of an autonomous system, while underwater, is extremely desirable.

Different approaches to establish such system have been proposed over the years. They include Short BaseLine (SBL), Long BaseLine (LBL), Ultra-Short BaseLine (USBL), GPS Intelligent Buoys (GIB) and some hybrid system based on the previous ideas [2]-[4].

All of those systems make use of acoustic signal travel time measurements to estimate the distance and in some systems the bearing, from the underwater vehicle to reference points, located on the surface or on the sea floor. Those systems are reliable when the depth being explored is on the order of or larger than the horizontal distances between the acoustic nodes.

Estimation of horizontal distances in relatively shallow water is a difficult task mainly due the multipath nature of the

propagation, where multiple arrivals reach the receiver at different times by different propagation paths, making it difficult to estimate accurately the time of arrival of the acoustic signals and consequently the distance.

This work intends to explore such environments presenting a technique to enhance the navigational and positioning accuracy of UUVs by networking a number of USVs utilizing underwater acoustic modems to measure acoustic travel times.

Travel time measurements are basically done by cross-correlating (or matched filtering) the received signal (echo) with a replica of the transmitted signal. The two-way travel time can then be estimated from the time lag where the peak in the cross-correlation (or matched filter output) occurs. This approach has been extensively studied [5]-[7].

The challenge is to develop an accurate estimate of the distance based on the travel time. In an environment where the speed of propagation is approximately constant, the distance can be estimated by a simple multiplication of the one-way travel time (half of the two-way travel time) and the characteristic medium sound speed. However, in underwater acoustic propagation, the sound speed varies spatially, as characterized in Fig. 1, making the simple multiplication a rough estimate.

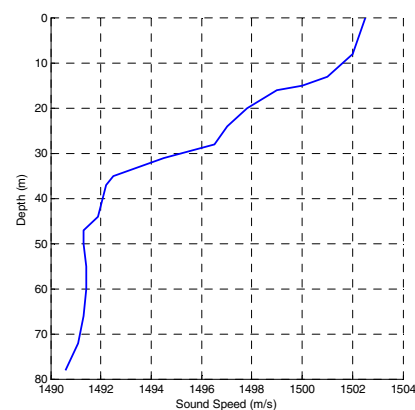


Fig. 1. Sound speed profile measured in Monterey Bay on August, 12<sup>th</sup> 2015

In general, a more accurate estimation for the distance can be generated by using an acoustic ray tracing algorithm to generate a prediction of the acoustic channel impulse response. This prediction can then be matched with the measured channel impulse response [8] by adapting the range in the ray tracing algorithm.

After determination of the range between the source (located on the UUV) and multiple receivers at known GPS coordinates (located on the USVs), each obtained at different times, a tracking algorithm was employed to estimate the UUV position. In previous work [1], a tracking algorithm based on the Extended Kalman Filter (EKF) was developed presenting satisfactory results.

An in-depth analysis of the tracking algorithm indicates that the assumption of the errors being Gaussian and zero mean at the base of the EKF is violated by the presence of nonlinearities in the measurement equation. Because of that, a more suitable approach based on the Unscented Kalman Filter (UKF) was taken. The new tracking algorithm (based on the UKF) yields improved tracking properties with reasonable computational effort.

## II. IMPROVED RANGE ESTIMATION BY ACOUSTIC CHANNEL MODELING

### A. Two-way travel time measurements

In this work, Teledyne-Benthos ATM-900 series acoustic modems have been used. The modems have a built-in ranging routine that makes use of a Doppler tolerant waveform (HFM pulse) to estimate the acoustic travel time. The HFM pulse has the following basic characteristics: 50 ms duration, 9 to 14 kHz bandwidth.

The basics of the Teledyne-Benthos built-in ranging routine can be described as follows. Consider a situation where two stationary modems are separated by the slant range  $R$ , and modem-1 requests a range to modem-2, as indicated in Fig. 2.

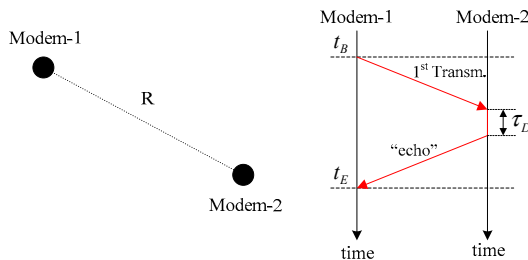


Fig. 2. Teledyne-Benthos Ranging Routine (adapted from [9])

Initially, modem-1 transmits via MFSK (Multiple Frequency Shift Keying) a utility package to modem-2 preceded by a HFM-pulse, recording the time where the routine starts,  $t_B$ . A matched filter in modem-2 detects the incoming signal and estimates the time of arrival based on the *highest peak* in the matched filter output. Modem-2 then replies to the range request after a known time delay  $\tau_D$ , sending a MFSK message (“echo”) containing the time delay

(and other information not important for ranging purposes) preceded by a HFM-pulse. Modem-1 now detects the incoming signal, and again estimates the time of arrival,  $t_E$ , by the *highest peak* in the matched filter output. From the time difference between  $t_E$  and  $t_B$  (minus  $\tau_D$ ), the two-way travel time is estimated by modem-1 [9] [10]. The one-way travel time ( $t_{ma}$ ) is just the half of the two-way travel time. It is worth noting that if the acoustic propagation between the two nodes were dominated by a direct path, corresponding to the shortest propagation path, then the highest peak in the matched filter would provide a very good estimate of the slant range (possibly neglecting a minor correction due to path curvature). Of interest in the shallow water environment being discussed here are geometries in which the dominant propagation path is not a direct path.

### B. Acoustic channel modeling and impulse response estimation

Sound speed profile, bathymetry characteristics and bottom properties can be easily incorporated into a propagation model using a ray tracing algorithm [11].

Considering a single source and receiver, the formulation of the ray theory in the time domain permits a fast assessment of the ideal acoustic channel complex impulse response (amplitude and phase of the eigenrays) [11] [12]. The ideal complex impulse response can then be used to construct the synthetic received signal. Following [13], the synthetic received signal is

$$x'(t) = \sum_{m=1}^M A_{R_m} x(t - \tau_m) - A_{I_m} \hat{x}(t - \tau_m), \quad (1)$$

where  $A_{R_m}$ ,  $A_{I_m}$ , and  $\tau_m$  are the real component of the complex amplitude, the imaginary component of the complex amplitude, and travel time of the  $m^{\text{th}}$  eigenray, respectively.  $M$  is the total number of contributing eigenrays,  $x(t)$  represents the transmitted signal and  $\hat{x}(t)$  is the Hilbert transform of the transmitted signal.

Assuming that the transmitted waveform autocorrelation has an impulse-like behavior, we can consider the matched filter output as the impulse response estimator for the acoustic channel [14]. Therefore, matched filtering the signal constructed using Eq. (1) (after basebanding) can produce a prediction for the channel impulse response (Fig. 3). We shall denote the time of the highest peak  $t_m$ .

In section II-A, it was seen that the one-way travel time ( $t_{ma}$ ) calculated by the Teledyne-Benthos acoustic modems is based on the time of the highest peak in the matched filter output.

The predicted channel impulse response can be then used iteratively (adjusting the horizontal range) to match the measured channel impulse response (measured by the acoustic modems) with one caveat: instead of trying to match the entire

time series, only the arrival with the highest amplitude will be matched (section II-A).

This approach is fast enough to run in dedicated hardware in real time. It yields a more accurate estimate of the range than just a multiplication of the one-way travel time with the characteristic medium sound speed. Residual errors will be small enough to be handled by the tracking algorithm, as will be described in section III.

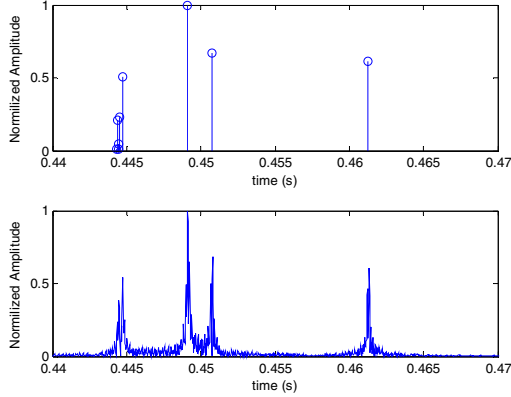


Fig. 3. Top: Ideal Impulse response from Bellhop, bottom: Predicted channel impulse response

### III. TRACKING ALGORITHM

The basis for the development of the EKF/UKF is to define, as accurately as possible, the state and measurement equations. Assuming that the UUV's speed through the water ( $V$ ), pitch ( $\phi$ ), heading ( $\theta$ ) and depth ( $d$ ) are known, a coordinate system where latitude and longitude are mapped to Cartesian coordinates can be built.

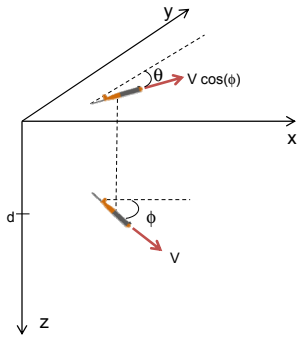


Fig. 4. Coordinate system for the state space equation

Based on the coordinate system, a kinematic model can be represented as

$$\begin{bmatrix} \dot{x}(t) \\ \dot{y}(t) \\ \dot{C}_x(t) \\ \dot{C}_y(t) \end{bmatrix} = \underbrace{\begin{bmatrix} 0 & 0 & 1 & 0 \\ 0 & 0 & 0 & 1 \\ 0 & 0 & 0 & 0 \\ 0 & 0 & 0 & 0 \end{bmatrix}}_A \underbrace{\begin{bmatrix} x(t) \\ y(t) \\ C_x(t) \\ C_y(t) \end{bmatrix}}_{X(t)} + \underbrace{\begin{bmatrix} 1 & 0 \\ 0 & 1 \\ 0 & 0 \\ 0 & 0 \end{bmatrix}}_B V(t) \cos(\phi(t)) \underbrace{\begin{bmatrix} \sin(\theta(t)) \\ \cos(\theta(t)) \end{bmatrix}}_{u(t)} + \underbrace{\begin{bmatrix} \epsilon_x \\ \epsilon_y \\ \epsilon_{C_x} \\ \epsilon_{C_y} \end{bmatrix}}_{v(t)}, \quad (2)$$

where  $C_x$  and  $C_y$  represent the velocity of the current in  $x$  and  $y$  directions, respectively.

After discretization assuming a suitable sampling interval  $\Delta t$ , the standard discrete time state equation can be written as

$$X(t + \Delta t) = \underbrace{(I + A\Delta t)}_F X(t) + \underbrace{\frac{B\Delta t}{G} u(t)}_G + v(t)\Delta t. \quad (3)$$

This leads to a discrete time signal model (state equation) as

$$X(k+1) = F X(k) + G u(k) + v(k). \quad (4)$$

Measurement equation: Assuming that the horizontal far-field beam pattern of the acoustic transducer is nearly omnidirectional, every measurement represents a circle of possible UUV position (range only measurements) [15].

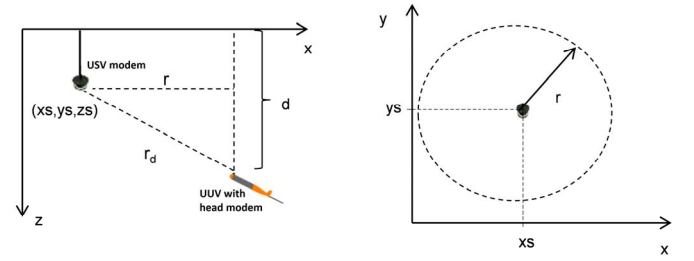


Fig. 5. Measurement model

The circle of possible UUV position is

$$(x - x_s)^2 + (y - y_s)^2 = r^2. \quad (5)$$

Expanding and rearranging the terms yields

$$r^2 - x_s^2 - y_s^2 = x^2 - 2x \cdot x_s - 2y \cdot y_s + y^2. \quad (6)$$

Therefore, the measurement equation can be written as

$$z(k) = h[k, x_k] + \omega(k), \quad (7)$$

where  $\omega(k)$  represents measurement noise, and

$$h[k, x_k] = x(k)^2 - 2x(k)x_s(k) - 2y(k)y_s(k) + y(k)^2. \quad (8)$$

At this point we have a linear state equation (4) and a non-linear measurement equation (7).

#### A. Extended Kalman Filter

The Extended Kalman filter uses Taylor series approximations for the non-linearities in the state and measurement equations. In our case, only the measurement equation (7) is non-linear and a first order Taylor series expansion can be used to linearize it as follows:

$$h(k, x_k) = h(k, \hat{x}_{k|k-1}) + H_k (x_k - \hat{x}_{k|k-1}), \quad (9)$$

where  $H_k = \frac{\partial h(k, x)}{\partial x} \bigg|_{x=\hat{x}_{k|k-1}}$ .

From Equations (7) and (8)

$$z(k) = H_k x_k + \omega(k) + h(k, \hat{x}_{k|k-1}) - H_k \hat{x}_{k|k-1}. \quad (10)$$

Note that, in this approach, the non-linear measurement equation needs to be differentiable. Fortunately, this condition is satisfied in this case.

Following [16], the Extended Kalman filter algorithm executes the following operations at each step  $k$ :

a) Prediction:

$$\hat{x}_{k+1|k} = F(k) \hat{x}_{k|k} + G(k) u(k). \quad (11)$$

$$P_{k+1|k} = F(k) P_{k|k} F(k)' + Q_k, \quad (12)$$

where  $Q$  represents the covariance of the Plant noise

b) Measurement update:

$$\hat{x}_{k|k} = \hat{x}_{k+1|k} + K_k (z_k - h(k, \hat{x}_{k+1|k})). \quad (13)$$

$$P_{k|k} = (I - K_k H_k) P_{k+1|k} (I - K_k H_k)' + K_k R_k K_k', \quad (14)$$

where  $K_k = P_{k+1|k} H_k' (H_k P_{k+1|k} H_k' + R_k)^{-1}$ ,  $R$  is the covariance of the measurement noise, and  $z_k = r^2 - xs^2 - ys^2$  as in Eq. (6).

### B. Unscented Kalman Filter

The Unscented Kalman Filter [17] is a technique that utilizes the unscented transform [18] and can be applied in models of the form of Equations (4) and (7). Instead of using linear approximations, as EKF requires, the idea of the unscented transform is to deterministically choose a fixed number of *sigma* points that capture the mean (state) and covariance of the original distribution. These sigma points are then propagated through the non-linearity, and the mean and covariance of the transformed variable are estimated from them.

Following [19] the Unscented Kalman filter algorithm executes the following operations at each step  $k$ :

a) Prediction:

- Form sigma points

$$\begin{aligned} \chi_{k-1}^{(0)} &= \hat{x}_{k|k}, \\ \chi_{k-1}^{(i)} &= \hat{x}_{k|k} + \sqrt{n+\lambda} \left[ \sqrt{P_{k|k}} \right]_i, \\ \chi_{k-1}^{(i+n)} &= \hat{x}_{k|k} - \sqrt{n+\lambda} \left[ \sqrt{P_{k|k}} \right]_i, \quad i = 1, \dots, n, \end{aligned} \quad (15)$$

where the matrix square root denotes a matrix such that  $\sqrt{P} \sqrt{P}' = P$ ,  $n$  is the length of the state,  $[\cdot]_i$  denotes the  $i^{\text{th}}$  column of the matrix and  $\lambda$  is a scaling parameter defined as  $\lambda = \alpha^2 (n + \kappa) - n$ . The parameters  $\alpha$  and  $\kappa$  determine the spread of the sigma points around the mean.

- Propagate the sigma points through the dynamic model

$$\hat{\chi}_k^{(i)} = F(k) \chi_{k-1}^{(i)} + G(k) u(k), \quad i = 0, \dots, 2n. \quad (16)$$

- Compute the predicted state and covariance

$$\hat{x}_{k+1|k} = \sum_{i=0}^{2n} W_i^{(m)} \hat{\chi}_k^{(i)}. \quad (17)$$

$$P_{k+1|k} = \sum_{i=0}^{2n} W_i^{(c)} (\hat{\chi}_k^{(i)} - \hat{x}_{k+1|k}) (\hat{\chi}_k^{(i)} - \hat{x}_{k+1|k})' + Q_k, \quad (18)$$

where the weights  $W_i^{(m)}$  and  $W_i^{(c)}$  are defined as

$$\begin{aligned} W_0^{(m)} &= \frac{\lambda}{n + \lambda}, \\ W_0^{(c)} &= \frac{\lambda}{n + \lambda} + (1 - \alpha^2 + \beta), \\ W_i^{(m)} &= \frac{1}{2(n + \lambda)}, \quad i = 1, \dots, 2n, \\ W_i^{(c)} &= \frac{1}{2(n + \lambda)}, \quad i = 1, \dots, 2n. \end{aligned} \quad (19)$$

$\beta$  is a parameter that can be used to incorporate prior information on the (non-Gaussian) distribution of the states.

b) Measurement update:

- Form the sigma points

$$\begin{aligned} \chi_k^{(0)} &= \hat{x}_{k+1|k}, \\ \chi_k^{(i)} &= \hat{x}_{k+1|k} + \sqrt{n+\lambda} \left[ \sqrt{P_{k+1|k}} \right]_i, \\ \chi_k^{(i+n)} &= \hat{x}_{k+1|k} - \sqrt{n+\lambda} \left[ \sqrt{P_{k+1|k}} \right]_i, \quad i = 1, \dots, n. \end{aligned} \quad (20)$$

- Propagate the sigma points through the measurement model

$$\hat{z}_k^{(i)} = h(k, \chi_k^{(i)}), \quad i = 0, \dots, 2n. \quad (21)$$

- Compute the predicted measurement mean  $\mu_k$ , covariance of the measurement  $S_k$ , and cross-covariance of the state and measurement,  $C_k$

$$\mu_k = \sum_{i=0}^{2n} W_i^{(m)} \hat{z}_k^{(i)} . \quad (22)$$

$$S_k = \sum_{i=0}^{2n} W_i^{(c)} (\hat{z}_k^{(i)} - \mu_k)(\hat{z}_k^{(i)} - \mu_k)' + R_k . \quad (23)$$

$$C_k = \sum_{i=0}^{2n} W_i^{(c)} (\chi_k^{(i)} - \hat{x}_{k+1|k})(\hat{z}_k^{(i)} - \mu_k)' . \quad (24)$$

- Compute the updated state and covariance

$$\hat{x}_{k|k} = \hat{x}_{k+1|k} + K_k (z_k - \mu_k) , \quad (25)$$

$$P_{k|k} = P_{k+1|k} - K_k S_k K_k' , \quad (26)$$

where  $K_k = C_k S_k^{-1}$  and  $z_k$  is given by Eq. (7)

As seen, the UKF is not based on a linear approximation at a single point as the EKF, but uses further points in approximating the non-linearity. Also the models for the system (state and measurement equations), when non-linear, are not required to be differentiable. Therefore, it's not necessary to calculate the gradient as in Eq. (9). On the other hand, the UKF requires a higher computational effort when compared with the EKF.

#### IV. COMPUTER SIMULATIONS

A combination of the EKF and UKF with a Smoothing Algorithm was developed and extensively tested with synthetic data. In the model built for the simulations, the position of the reference points (at known GPS locations), acting in Fig.6 as sensors, and the UUV trajectory are parameters that can be modified, permitting the study of different geometries. Additionally, a failure in a certain sensor, as well as noise, can be added in the model permitting evaluation of such effects for a more realistic scenario.

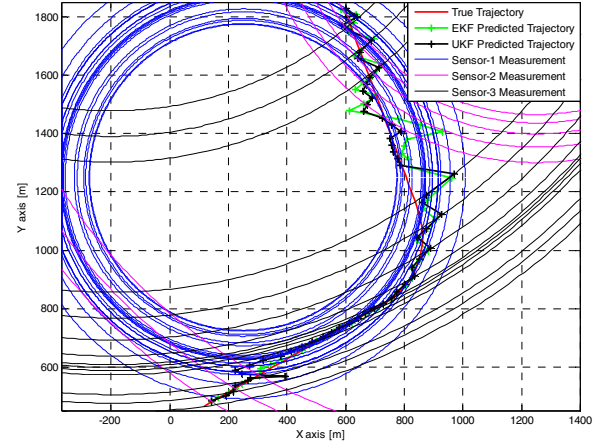
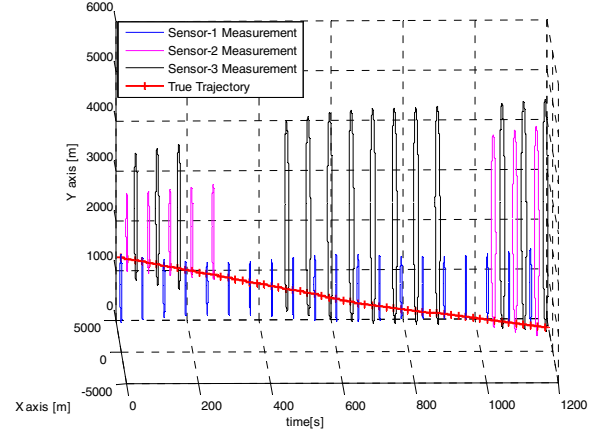


Fig. 6. Simulation results

On the top of Fig. 6, the time evolution of the measurements can be seen, as well as the lack of measurement of sensors 2 and 3 in certain intervals. The bottom plot shows the measurements and how the predicted trajectories are consistent with the true trajectory. In Fig. 7, a comparison between smoothed and predicted trajectories can be seen, and in Fig. 8 the errors can be analyzed.

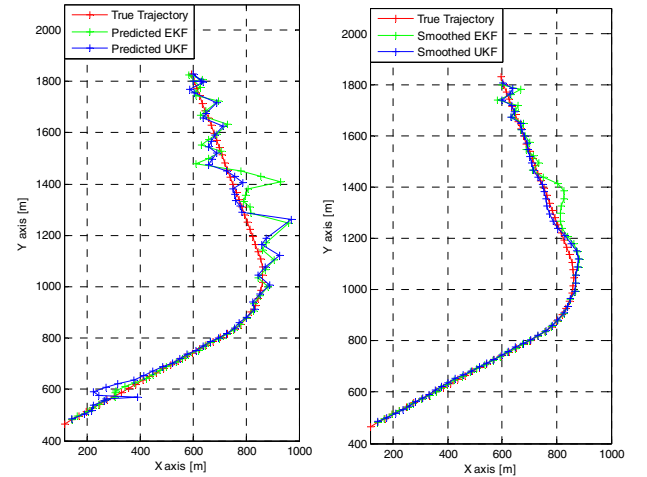


Fig. 7. Predicted and smoothed trajectories



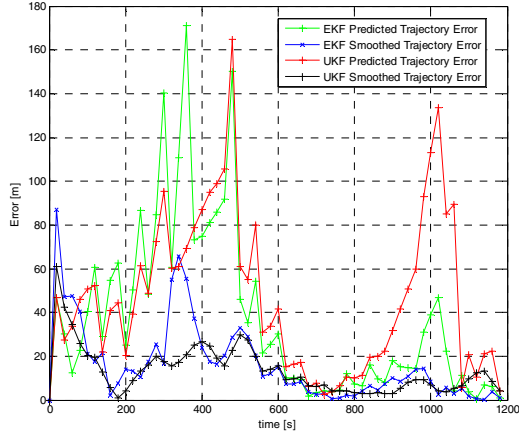


Fig. 8. Error analysis

## V. SEA TESTS

In a one-week sea test, two Liquid Robotics Wave Gliders (USVs) named Mako and Tiburon, a Command Ship (NOAA R/V Fulmar), and an Alaska Native Tech. Littoral Glider (UUV) named LG16, all equipped with Teledyne-Benthos acoustic modems, were employed to obtain such tracking data. The objective of the sea test was to evaluate the algorithm's ability to track the UUV using the built-in acoustic ranging routine in the Teledyne-Benthos modems.

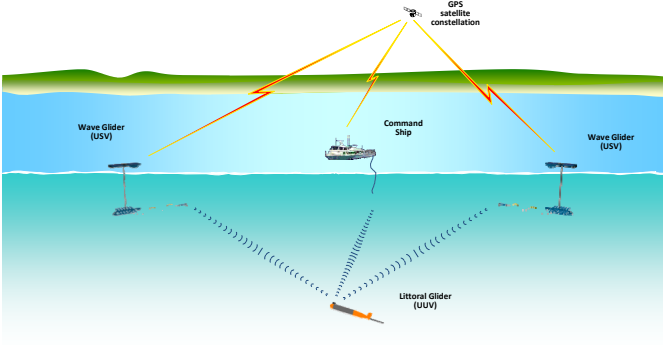


Fig. 9. Sea test mission

The built-in ranging routine makes use of HFM pulses and matched filters to estimate the travel times between the UUV and the surface assets equipped with the same type of modem. Through GPS measurements, each of the surface assets are at known locations. The travel times measured by the Benthos modems were converted to ranges by matching the impulse responses as described in section II. These ranges were then used as inputs into the tracking algorithm.

During the sea tests, several one-hour missions were successfully conducted. For each mission, the UUV navigation system recorded its position predictions and, because of its simplicity, errors of the order of 500 meters and above were observed between the final UUV predicted position and its GPS location, measured soon after it surfaced. In parallel,

several travel time measurements between the UUV and the other assets were successfully recorded (Fig. 10).

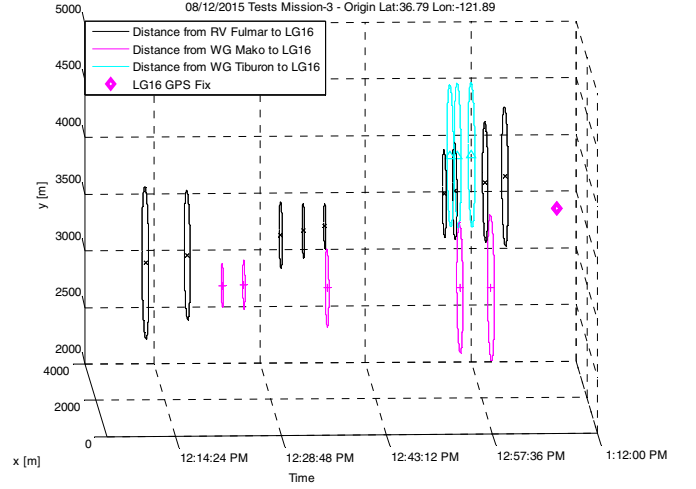


Fig. 10. Distance Measurements between the assets

For this particular mission, tracking by dead reckoning yielded errors of the order of 500 meters (Fig 11). The proposed tracking algorithm was tested and the results show a more accurate predicted position for the entire UUV trajectory.

When a rough estimate for the range is used (multiplication of the one-way travel time by the characteristic medium sound speed) errors around 35 meters were observed at the end of the mission. While this is an improvement, it does not account for the multipath effects of the propagation.

When the more complete algorithm described in this work is utilized, the final error is reduced to around 15 meters for EKF and 8 meters for UKF based algorithm (Figures 11 and 12). Thus, the impact of correlating the measured impulse response of the channel with a ray trace prediction provides an improvement in the tracking accuracy.

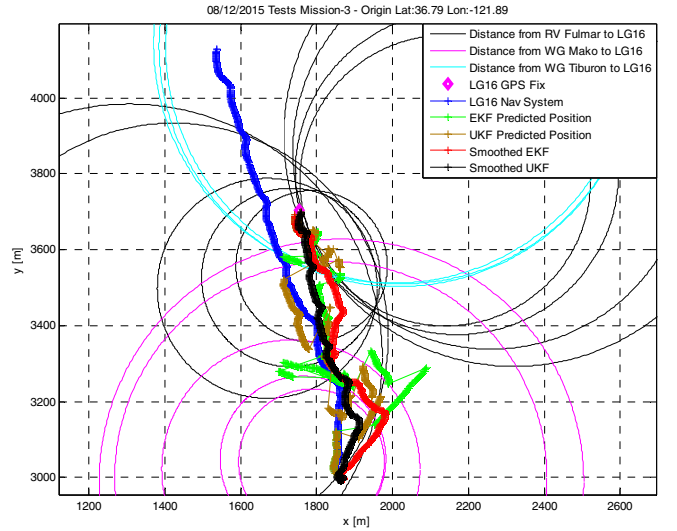


Fig. 11. Distance Measurements between the assets and tracking results

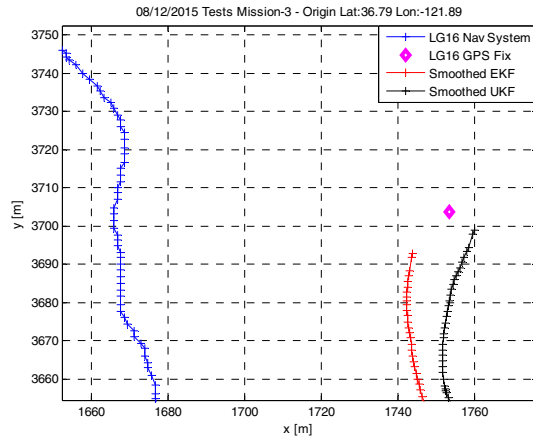


Fig. 12. Last tracking predictions using UKF and EKF

## VI. CONCLUSIONS AND FUTURE WORK

Results of the sea tests confirm that the developed tracking algorithm, based on the Kalman Filter and incorporating range estimates from acoustic modems, is able to improve the navigation accuracy of underwater vehicles.

The tracking algorithm based on the UKF, due to its better treatment of the non-linearity in the measurement equation, was able to provide an improved tracking estimate when compared with the EKF version. Another advantage of the UKF based algorithm is that the non-linear equation does not need to be differentiable. On the other hand, UKF requires a higher computational effort. In our case, due to the small number of variables in the state, this proved not to be a limiting factor.

An important aspect to be examined in the future is the inclusion of the transmitter and receiver beam patterns in the predicted impulse response modeling. This may provide more accurate range estimates between the assets employed in the sea test.

## ACKNOWLEDGMENT

The authors gratefully acknowledge the support of the Naval Postgraduate School Consortium for Robotics and Unmanned Systems Education and Research (CRUSER), Office of Naval Research, and the Brazilian Navy. The authors also wish to thank our colleagues at Teledyne-Benthos for numerous discussions about the ranging algorithm utilized in their modems.

## REFERENCES

- [1] R. P. Vio, R. Cristi, and K. Smith, "Near real-time improved UUV positioning through channel estimation", 2016. Proc. of UComms Conference, La Spezia, Italy, Sept, 2016 (in press).
- [2] P. H. Milne, Underwater Acoustic Positioning Systems, Gulf Publishing Company, 1983.
- [3] J. Vaganay, J. J. Leonard, J. A. Curcio and J. S. Willcox, "Experimental Validation of the Moving Long Base-Line Navigation Concept," in Autonomous Underwater Vehicles, IEEE-OES, 2004.

- [4] A. Alcocer, P. Oliveira and A. Pascoal, "Underwater Acoustic Positioning System Based on Buoys with GPS," in Eighth European Conference on Underwater Acoustics, 8th ECUA, 2006.
- [5] G. C. Carter, *Coherence and time delay estimation: an applied tutorial for research, development, test, and evaluation engineers*. IEEE Press, 1993.
- [6] C. H. Knapp and G. C. Carter, "The generalized correlation method for estimation of time delay". IEEE trans. on acoustics, speech, and signal processing N. 4, 1976.
- [7] J. P. Ianniello, "Time delay estimation via cross-correlation in the presence of large estimation errors". IEEE trans. on acoustics, speech, and signal processing N. 6, 1982.
- [8] Z. H. Michalopoulou, "Matched-impulse processing for shallow-water localization and geoacoustic inversion". Journal of Acoustic Society of America N. 108, 2000.
- [9] M. J. Hahn, Undersea navigation via distributed acoustic communications network, Monterey: Master Thesis, Naval Postgraduate School, 2005.
- [10] D. Green, Teledyne-Benthos, Personal Communication, April, 2015.
- [11] M. Porter, "The BELLHOP manual and user's guide: Preliminary draft". Ocean Acoustics Library, 2011 <http://oalib.hlsresearch.com/>
- [12] M. Porter and H. Bucker, "Gaussian beam tracing for computing ocean acoustic fields". Journal of Acoustic Society of America N. 82, 1987.
- [13] F. B. Jensen, W. A. Kuperman, M. B. Porter and H. Schmidt, *Computational Ocean Acoustics*, 2<sup>nd</sup> Edition, Springer, 2011.
- [14] M. I. Taroudakis, G. N. Makrakis (editors), *Inverse Problems in Underwater Acoustics* (Chapter 5). Springer-Verlag New York, Inc., 2001.
- [15] J. Djughash, S. Singh and P. Corke, "Further results with localization and mapping using range from radio". Field and Service Robotics, STAR 25, pp. 231-242, 2006.
- [16] Y. Bar-Shalom, X. Rong Li and T. Kirubarajan, *Estimation with applications to tracking and navigation, chapter 10*. John Wiley & Sons, Inc., 2001.
- [17] S. Julier, J. K. Uhlmann, and Durrant-Whyte, H. F. "A new approach for filtering nonlinear systems". Proceedings of the 1995 American Control Conference. Seattle, Washington.
- [18] S. Julier and J. K. Uhlmann, "A general method for approximating nonlinear transformations of probability distributions". Tech. rept. Robotics research group, Department of Eng. Sciences, University of Oxford, 1996.
- [19] S. Sarkka, *Bayesian Filtering and Smoothing*. Cambridge University Press, 2013.